

Research Article

Enhancing Performance of SnO₂-Based Dye-Sensitized Solar Cells Using ZnO Passivation Layer

W. M. N. M. B. Wanninayake,^{1,2} K. Premaratne,^{2,3} and R. M. G. R. Rajapakse^{2,4}

¹Department of Civil Engineering, Faculty of Engineering, University of Peradeniya, 20400 Peradeniya, Sri Lanka

²Postgraduate Institute of Science, University of Peradeniya, 20400 Peradeniya, Sri Lanka

³Department of Physics, Faculty of Science, University of Peradeniya, 20400 Peradeniya, Sri Lanka

⁴Department of Chemistry, Faculty of Science, University of Peradeniya, 20400 Peradeniya, Sri Lanka

Correspondence should be addressed to W. M. N. M. B. Wanninayake; mihira.wanninayake@gmail.com

Received 11 August 2016; Revised 6 September 2016; Accepted 8 September 2016

Academic Editor: Yanfa Yan

Copyright © 2016 W. M. N. M. B. Wanninayake et al. This is an open access article distributed under the Creative Commons Attribution License, which permits unrestricted use, distribution, and reproduction in any medium, provided the original work is properly cited.

Although liquid electrolyte based dye-sensitized solar cells (DSCs) have shown higher photovoltaic performance in their class, they still suffer from some practical limitations such as solvent evaporation, leakage, and sealing imperfections. These problems can be circumvented to a certain extent by replacing the liquid electrolytes with quasi-solid-state electrolytes. Even though SnO₂ shows high electron mobility when compared to the semiconductor material commonly used in DSCs, the cell performance of SnO₂-based DSCs is considerably low due to high electron recombination. This recombination effect can be reduced through the use of ultrathin coating layer of ZnO on SnO₂ nanoparticles surface. ZnO-based DSCs also showed lower performance due to its amphoteric nature which help dissolve in slightly acidic dye solution. In this study, the effect of the composite SnO₂/ZnO system was investigated. SnO₂/ZnO composite DSCs showed 100% and 38% increase of efficiency compared to the pure SnO₂-based and ZnO-based devices, respectively, with the gel electrolyte consisting of LiI salt.

1. Introduction

Dye-sensitized solar cells (DSCs) based on thin film nanocrystalline high band gap semiconductor materials have received attention as an alternative to conventional single-crystal silicon solar cells owing to their low production cost, easy fabrication procedure, and relatively high energy-conversion efficiency. Since the early development of DSCs by Grätzel in 1991, considerable effort has been devoted to improving their performance [1, 2]. This study focused on the development of the semiconductor material and electrolyte as the efficiency of the DSCs depends on many factors such as semiconductor material, sensitizer, and electrolyte. In DSCs, TiO₂ is the most popular semiconductor material, but it shows some retarding effects due to its low electron mobility and charge transport property which leads to increase of the dark current of the solar cell device and photocatalytic ability which tends to degrade the dye molecules. Therefore, SnO₂ is employed in place of TiO₂ as it has $\sim 250 \text{ cm}^2 \text{ V}^{-1} \text{ s}^{-1}$ of

electron mobility [3, 4]. This property of SnO₂ will contribute towards recombination through the surface trap levels of SnO₂ nanoparticles. There are two major recombination processes present in DSCs. One is regeneration of excited dye molecules with the injected electrons. The other is combination of the injected electrons with the triiodide ions in the electrolytes due to the back tunneling of injected electrons.

In order to enhance the performance of the SnO₂-based solar cell device by reducing recombination effect, one of the useful methods is applying the ZnO coating layer on top of the SnO₂ surface. This ZnO layer also acts as a passivation layer which will reduce the I₃⁻ ion recombination with the injected electron. Since ZnO is a high band gap semiconductor it is expected to act in a different manner than the high band gap insulating coating layers. Kumara et al. have conducted a research based on composite SnO₂/ZnO system with liquid electrolytes and achieved an efficiency of 4.9%. As far as we are concerned, this is the first time that the

performance and suitability of composite SnO_2/ZnO with gel polymer electrolytes are reported [5–8].

Even though the use of gel polymer electrolytes sacrifices the performance of DSCs to some extent due to low ion mobility, it shows cohesive nature of solids and diffusive nature of liquids while showing good stability in outdoor applications due to their promising properties such as thermal stability, nontoxicity, lower flammability, and environmental friendliness. Generally, the diffusivity of triiodide ions in gel based electrolytes lies in 10^{-6} to 10^{-7} $\text{cm}^2 \text{s}^{-1}$ range. Electrolytes based on organic solvents or ionic liquids can be gelled or polymerized by dispersing suitable polymer materials to obtain quasi-solid-state electrolytes. Polymer backbone in gel electrolyte medium will help the transport of ions and this ion conduction is called the Grotthuss mechanism.

There is a vast amount of literature available for the DSCs fabricated with polymer based gel electrolytes and their effects on the performance of the device [9–20]. In summary, polymethylhydrosiloxane, poly(vinylidene fluoride-co-hexafluoropropylene) (PVDFHFP), 3-methoxypropionitrile (MPN), 2,4-di-O-dimethylbenzylidene-D-sorbitol (DMDBS), poly[di(ethylene glycol)-2-ethyl hexyl ether acrylate] (PDEA), poly(vinylpyridine-co-acrylonitrile) [P(VP-coAN)], poly(ethylene oxide) (PEO), polyvinylpyridine, hydroxystearic acid, imidazole polymers, polysaccharides, poly(epichlorohydrin-co-ethylene oxide), and polyacrylonitrile (PAN) polymers were used in the past few decades. Also, the other trend of gelatin mechanism is by the introduction of nanofillers such as TiO_2 , Al_2O_3 , fumed silica, and many other inorganic materials into the host liquid electrolytes. Somehow, these types of polymer based gel electrolytes gave an efficiency of about 7%. The conductivities of the gel polymer based electrolytes mainly depended on the oligomer size or molecular weight and salts used in the gel polymer electrolyte. LiI salt and PAN-based gel polymer [21] electrolytes are most frequently used in fabrication of DSCs in addition to mixed salts based gel electrolytes [22]. Therefore, this study is focused on developing the proper gel polymer electrolytes based on PAN and salts such as LiI and $\text{Pr}_4\text{N}^+\text{I}^-$ in addition to improving the performance of semiconductor material.

2. Method and Methodology

2.1. Preparation of ZnO Working Electrode. ZnO (Aldrich 99%, 0.60 g), acetic acid (Aldrich 98%, 5.50 cm^3), Triton X-100 (Aldrich 98%, 5 drops), and ethanol (Aldrich 98%, 40.0 cm^3) were mixed together and ground well and the resultant solution sonicated for 15 min. Next, the solution was sprayed onto an FTO glass ($10 \Omega \text{cm}^{-2}$) using spray pyrolysis technique at a temperature of 150°C and, subsequently, the sample was sintered at 500°C for 30 min and was allowed to cool down to 80°C . Then the sample was immersed in the dye solution (indoline D-358, 3×10^{-4} M in 1:1 volume ratio of acetonitrile/tert-butyl alcohol) for 12 hours. The same procedure was followed to prepare the SnO_2 -based DSCs through the use of colloidal SnO_2 (3.00cm^3) in place of ZnO.

2.2. Preparation of SnO_2/ZnO Composite Working Electrode. Colloidal SnO_2 (Alfa-Aesar, 3.00cm^3), acetic acid (Aldrich 98%, 10 drops), Triton X-100 (Aldrich 98%, 3 drops), ethanol (Aldrich 98%, 40.0 cm^3), and different amounts of ZnO (Aldrich > 97%, <50 nm), varying from 0.00 g to 0.10 g, were mixed thoroughly and the resulting SnO_2/ZnO suspensions were used separately to make devices with varying percentages of ZnO after undergoing ultrasonic treatment. In each case, the SnO_2/ZnO suspensions were sprayed onto well-cleaned FTO glass ($10 \Omega \text{cm}^{-2}$) plates heated to 150°C on a (preheated) hotplate. Then, all the samples were sintered at 500°C for 30 minutes and allowed to cool down to 80°C . The samples were then immersed in an indoline D-358 dye solution for 12 hours, and the dye coated- SnO_2/ZnO films were rinsed with acetonitrile to remove any physically adsorbed dye molecules. Next, the electrolyte was sandwiched between the FTO/ SnO_2/ZnO working electrode and a lightly platinized FTO counterelectrode ($\sim 7 \Omega/\text{sq}$, Aldrich) to assemble the solar cell device.

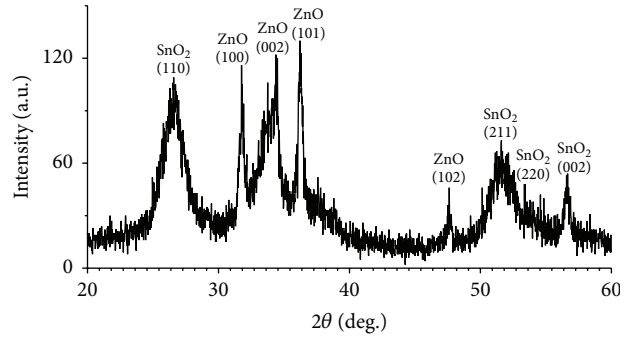
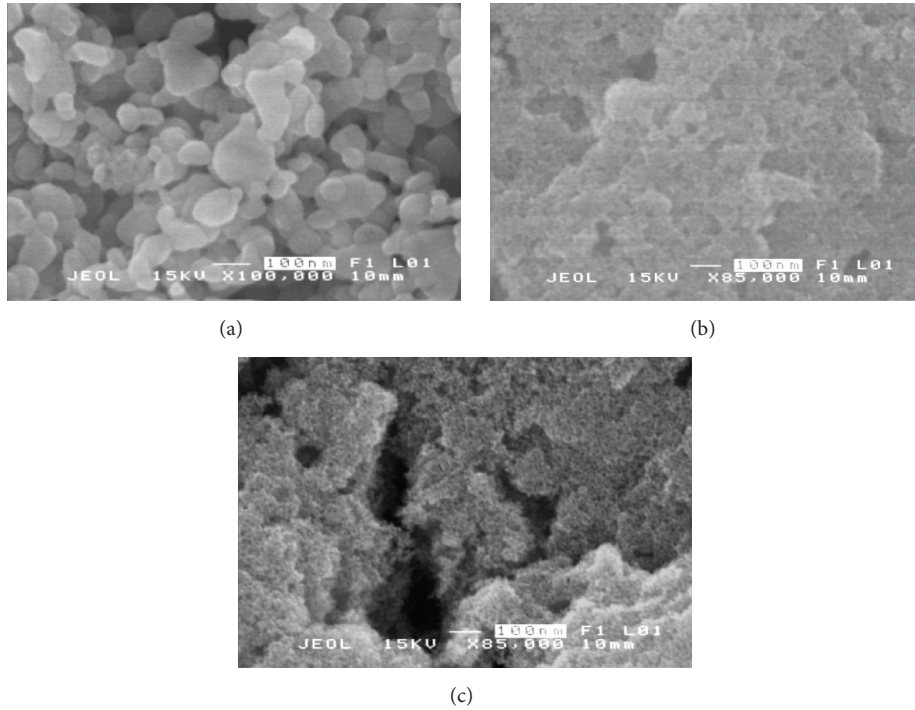
2.3. Preparation of Liquid Electrolyte. 1.55 g of dimethyl propyl imidazolium iodide, 0.65 g of 4-tert-butylpyridine (Aldrich 98%), 0.13 g of LiI (Aldrich 99%), 0.12 g of iodine (Aldrich 98%), and 7.59 g of acetonitrile (Aldrich 97%) were mixed well in an environment of nitrogen and purged with nitrogen for 14 hours.

2.4. Preparation of Gel Polymer Electrolytes. In this experiment, 0.225 g of polyacrylonitrile (Aldrich), 0.525 g of ethylene carbonate (Aldrich 98%), 0.750 g of propylene carbonate (Aldrich 99%), and 0.020 g of iodine (Aldrich 98%) were mixed and well stirred in a magnetic stirrer for 12 hours. 0.150 g of LiI (Aldrich 99%) (electrolyte Y) and 0.150 g of $\text{Pr}_4\text{N}^+\text{I}^-$ (Aldrich 98%) (electrolyte X) were used separately to prepare the gel electrolyte. Each time, the electrolytes were stirred at 80°C until the mixture turned into a clear, homogeneous, viscous gel. In each case, the gel electrolytes were subsequently pressed by sandwiching them between two clean glass plates to obtain a free-standing polymer film. They were subsequently dried in a vacuum desiccator overnight, at room temperature, to remove any absorbed moisture.

3. Results and Discussion

First, XRD spectrum was studied for the SnO_2/ZnO composite system in order to verify the presence of both materials. Respective plane values for each material were also identified and presented in XRD image as shown in Figure 1.

SEM images were obtained in order to study the morphology of the semiconductor film. Figure 2(a) gives evidence for enhancement of dye adsorption due to the increase of surface area, thus giving higher photocurrent density. Porous nature of ZnO film will also lead to better electrolyte penetration and also higher recombination. As these two factors are competing effects, through the result we obtained, we can conclude that most dominant factor in this situation is recombination effects. According to Figure 2(c), it shows suitable porous structure which can avoid negative effects due to electrolyte penetration into deep sites of the network.

FIGURE 1: XRD spectrum for SnO₂/ZnO composite system.FIGURE 2: SEM images of (a) ZnO, (b) SnO₂, and (c) SnO₂/ZnO composite systems.

The variation of solar cell parameters was observed with the variation of ZnO amount and observed results are depicted in Figure 3. The reasoning for this sinusoidal variation of V_{OC} and J_{SC} has been given in the next paragraph.

The results of J_{SC} and V_{OC} and efficiency of optimized composition of ZnO, SnO₂, and SnO₂/ZnO composite system have been given in Table 1 and Figure 4. When ZnO is used as the coating material, it is possible that ZnO, being a semiconducting material, would act in a different manner to insulating materials. For SnO₂/ZnO DSC, injected electrons from the excited dye molecules attached to ZnO outer layer would fill the conduction band of ZnO and then would be transferred to the conduction band of the SnO₂. According to conduction band positions of ZnO (−4.3 eV with respect to vacuum level) and SnO₂ (−5.0 eV with respect to vacuum level) and the results which were obtained for the SnO₂/ZnO composite system, the above assumption seems

to be more valid as the electrons try to move towards the lower energy, according to thermodynamics [23]. First, SnO₂/ZnO composite system showed lower V_{OC} and J_{SC} values due to the recombination occurring at uncovered sites of the SnO₂ network. When the amount of ZnO is increased, SnO₂ nanoparticles tend to become fully covered with ZnO nanoparticles and thereby the recombination occurring at the interfaces of dyed-SnO₂/electrolyte will be reduced. The reason is that the electrons in the conduction band of SnO₂ have a lesser possibility to reach the surface traps of the ZnO coating layer in order to recombine with triiodide ions or oxidized dye molecules. After the certain point of ZnO amount in Figure 3, V_{OC} and J_{SC} started to decrease. This is possibly due to the lower electron tunneling probability through ZnO coating layer as the higher ZnO amount will lead to increase the coating layer thickness [21].

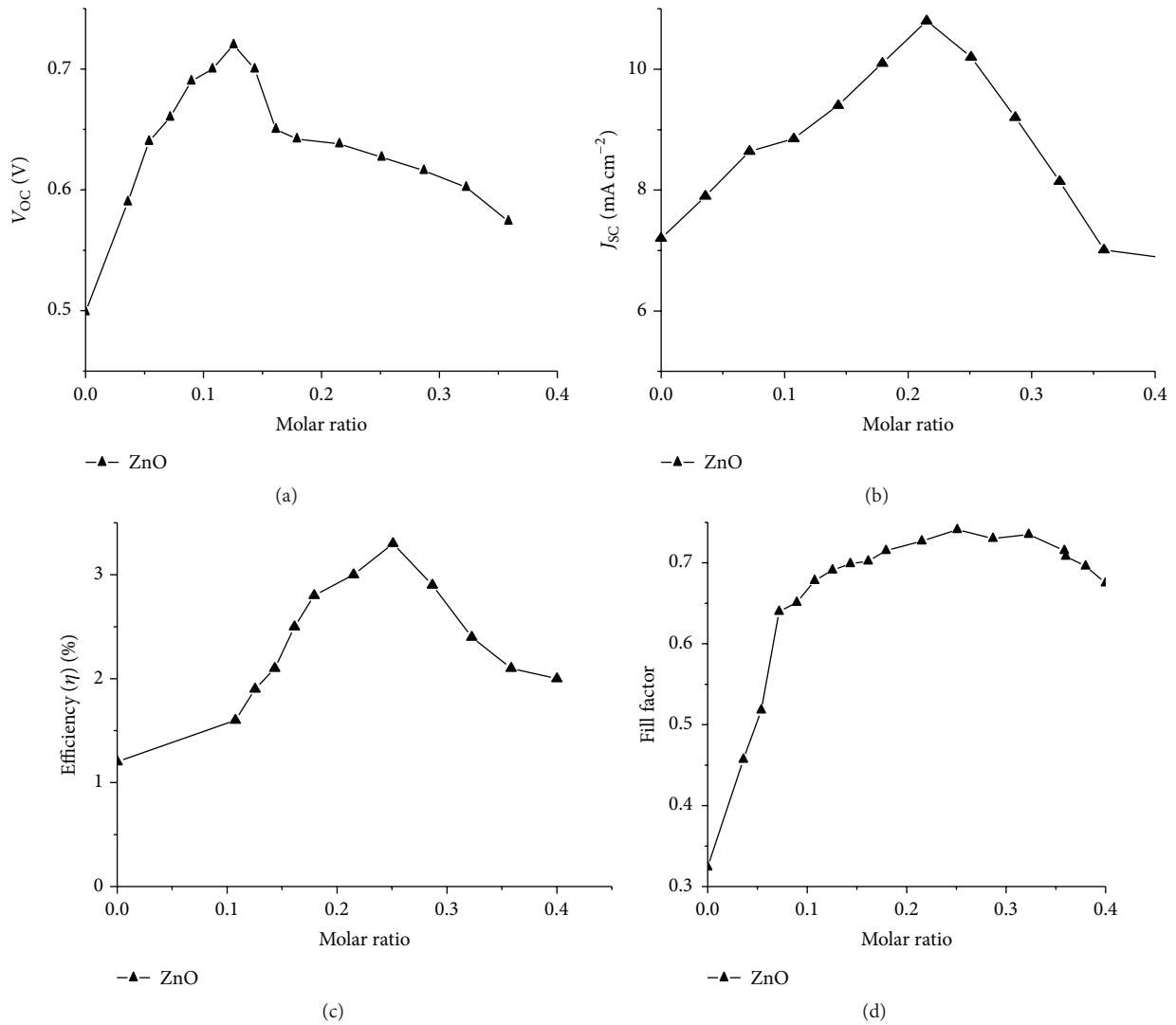


FIGURE 3: Variations of solar cell parameters of DSCs made using various compositions of ZnO-coated SnO₂ on with electrolyte X. Variation of (a) V_{OC} , (b) J_{SC} , (c) efficiency, and (d) fill factor, respectively, under 100 mW cm⁻² illumination.

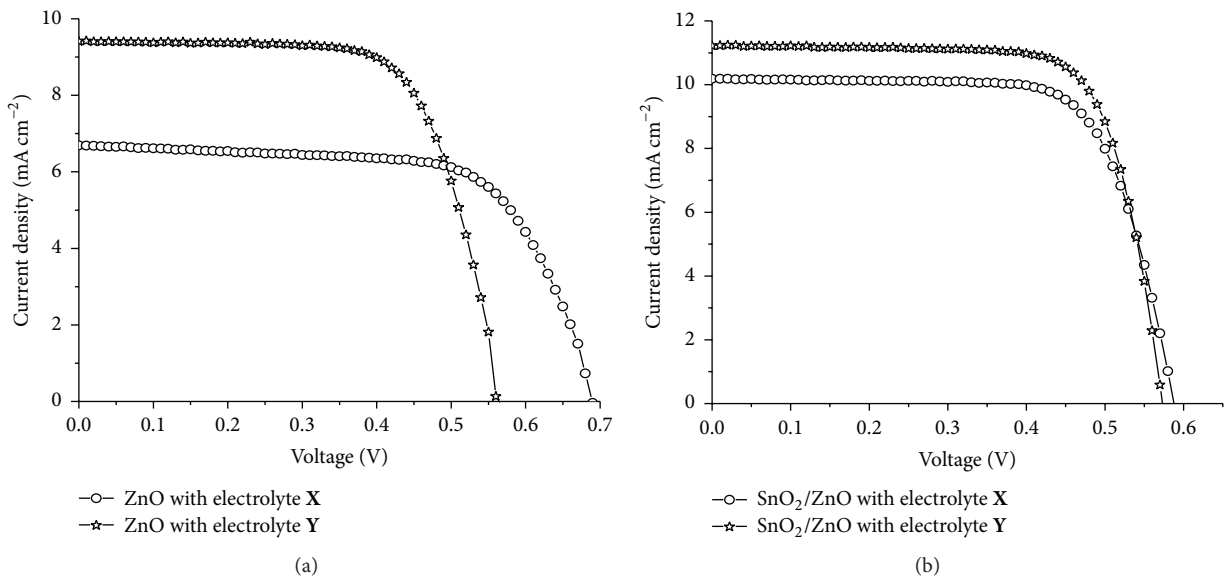


FIGURE 4: I-V characteristics curves of the QSDSCs fabricated with composite systems: (a) pure ZnO and (b) SnO₂/ZnO with electrolytes X and Y.

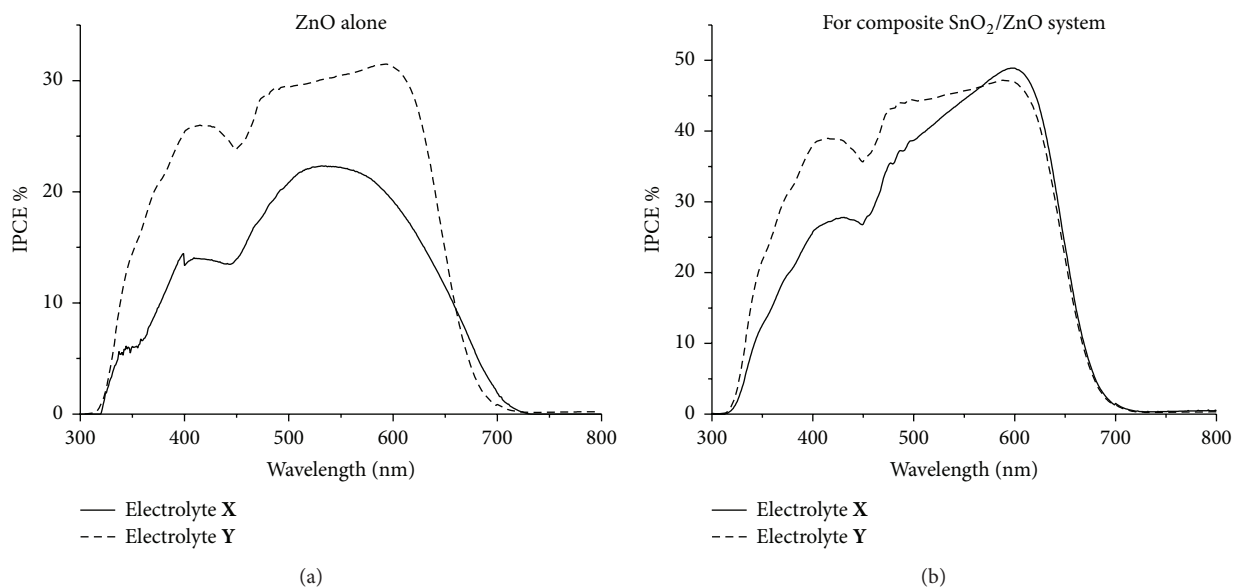


FIGURE 5: IPCE curves of the QSDSCs fabricated with composite systems: (a) ZnO alone and (b) SnO₂/ZnO with electrolytes X and Y.

TABLE 1: IV characteristics of SnO₂/ZnO composite DSCs.

Electrolyte	System	J_{SC} (mA cm ⁻²)	V_{OC} (V)	Fill factor	Efficiency%
X	SnO ₂	7.80	0.46	0.35	1.2
	ZnO	6.70	0.68	0.40	1.8
	SnO ₂ /ZnO	10.2	0.58	0.57	3.4
Y	SnO ₂	9.20	0.45	0.48	2.0
	ZnO	9.30	0.56	0.55	2.9
	SnO ₂ /ZnO	11.1	0.57	0.63	4.0
Liquid	SnO ₂ /ZnO	13.5	0.672	0.647	5.9

TABLE 2: Amount of dye adsorbed and bond distances.

System	Dye amount ($\times 10^{-5}$ mol L ⁻¹ cm ⁻²)	Distance between two consecutive cations (\AA)	Isoelectric point (\sim pH)
SnO ₂	4.00	Sn ⁴⁺ -Sn ⁴⁺ 3.2	5.5
SnO ₂ /ZnO	4.91	Zn ²⁺ -Zn ²⁺ 5.2	8.7
ZnO	4.70		10.0

The devices fabricated with the electrolyte containing Li⁺ ions showed higher J_{SC} and lower V_{OC} compared to those consisting of Pr₄N⁺ ions in the electrolyte. The presence of the Li⁺ ions increases the amorphous nature of the gel electrolyte due to the formation of cross-linking sites with polymer backbone, thus enhancing the diffusivity of the triiodide ions (for Li⁺ ion based electrolyte, 1.7×10^{-7} cm² s⁻¹, and for Pr₄N⁺ ion based electrolyte, 9.90×10^{-8} cm² s⁻¹). Li⁺ ions can be adsorbed onto the semiconductor surface, thus lowering the conduction band level of the semiconductor [22]. This effect will increase the J_{SC} while lowering V_{OC} . Since the Pr₄N⁺ ions do not contain lone-pair or low-lying empty orbitals, there is no possibility for adsorption of Pr₄N⁺ ions onto the semiconductor surface and V_{OC} values obtained also seem to agree with this argument. This has been reported by several workers on the behavior of LiI and Pr₄N⁺I⁻ as salts [24–26].

TABLE 3: Zeta potential values for SnO₂/ZnO composite system.

System	Zeta potential (mV)
SnO ₂	-18.4
SnO ₂ /ZnO	+28.3
ZnO	+35.0

Since IPCE measurements were done in short circuit conditions, this does not indicate the efficiency of the device which is given under AM 1.5 conditions as depicted in Figure 5. It gives an idea about J_{SC} of the device. IPCE value of the SnO₂/ZnO composite system with the electrolyte Y has shown a maximum value of about 50% in the wavelength range around 650 nm and it showed a much broader curve supporting its J_{SC} value. This might be due to the favorable bonding nature between ZnO and dye molecules which leads to increase in the electron injection efficiency.

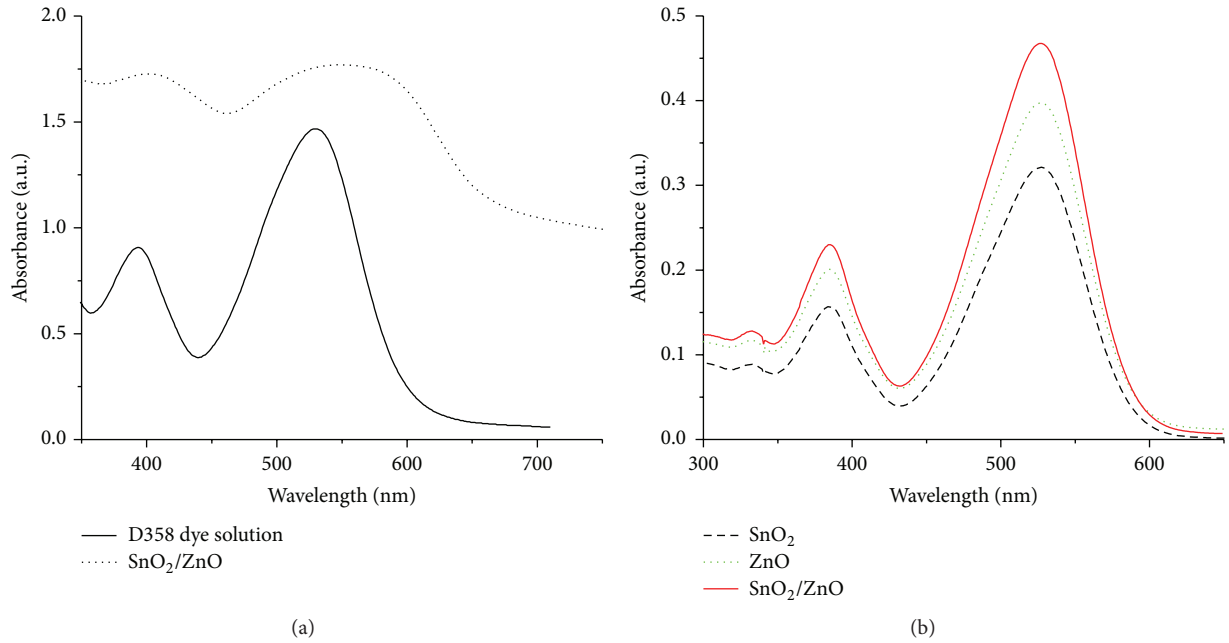


FIGURE 6: (a) UV-visible absorption spectra of indoline D358 dye in 1 : 1 volume ratio of acetonitrile/tert-butyl alcohol (solid line) and system consists of dye/ZnO/SnO₂ film on the FTO substrate (dotted line) and (b) disorbed dye solution from 1 cm × 1 cm films.

TABLE 4: Electron lifetime, charge transport time, chemical capacitance, and resistance values obtained for each composite system of the DSCs with electrolytes X and Y.

Electrolyte	System	R_s (Ω)	R_{ct} (Ω)	R_t (Ω)	C_μ (10^{-6} F)	τ_e (ms)	L_n (10^{-6} m)	D_e (10^{-9} m ² s ⁻¹)
X	SnO ₂ /ZnO	23	1640	76.0	30.0	49.2	79	127
	ZnO alone	8.0	1750	42.0	41.0	71.8	110	168
Y	SnO ₂ /ZnO	20	142	78.2	22.0	3.12	23.0	168
	ZnO alone	11	128	36.2	40.0	5.12	32.0	200

Tabulated results for distance between two consecutive cations and isoelectric point positively direct to the explanation of higher performance of SnO₂/ZnO-based DSCs as shown in Table 2. The distance between two consecutive COO⁻ groups of dye molecules is of about 7 Å. It will support the better anchorage of dye molecules with the SnO₂/ZnO system as the surface of SnO₂ is covered by the ZnO.

System with SnO₂ alone shows a -18.4 mV zeta potential value and it shows better-chelating ability when cations like Zn²⁺ are introduced to the system according to the results shown in Table 3. Increase of zeta potential value towards more positive potential will help forming a better interaction between the Zn²⁺ ions in the surface of the composite system and the COO⁻ groups of the dye molecules. This will lead to a better dye adsorption.

According to Figure 6, the absorption spectra for dyed SnO₂/ZnO composite films show significant broadening of the bands due to the better anchorage of dye molecules onto the composite surface. Also, these absorption spectra exhibit a bathochromic shift in the absorption maximum possibly due to J-aggregation of the sensitizer molecules. This might be the reason for the somewhat lower performance observed in SnO₂/ZnO-based DSCs.

The following quantities such as series resistance R_s , recombination resistance R_{ct} , transport resistance, R_t , and chemical capacitance C_μ are taken from Nyquist plots shown in Figure 7, by fitting an equivalent circuit which is shown in Figure 8. Lifetime of electron τ_e , effective diffusion length of electrons L_n , and diffusion coefficient of electrons D_e are calculated using standard formula [27, 28] and they are tabulated in Table 4.

Values obtained for C_μ and R_{ct} in electrolyte Y showed lower values than that of the electrolyte X. Due to the low recombination resistance, high recombination will take place in the system consisting of electrolyte Y, thus reducing V_{OC} of the devices. Adsorption of Li⁺ ions onto the semiconductor will lead to lower V_{OC} due to the lowering of the energy difference between the redox potential and the Fermi level as conduction band is moved downward.

4. Conclusion

ZnO coating layer will help increase the performance of SnO₂-based DSCs by reducing the back tunneling of electrons while efficiently helping the electron transfer towards lower energy levels according to the thermodynamics

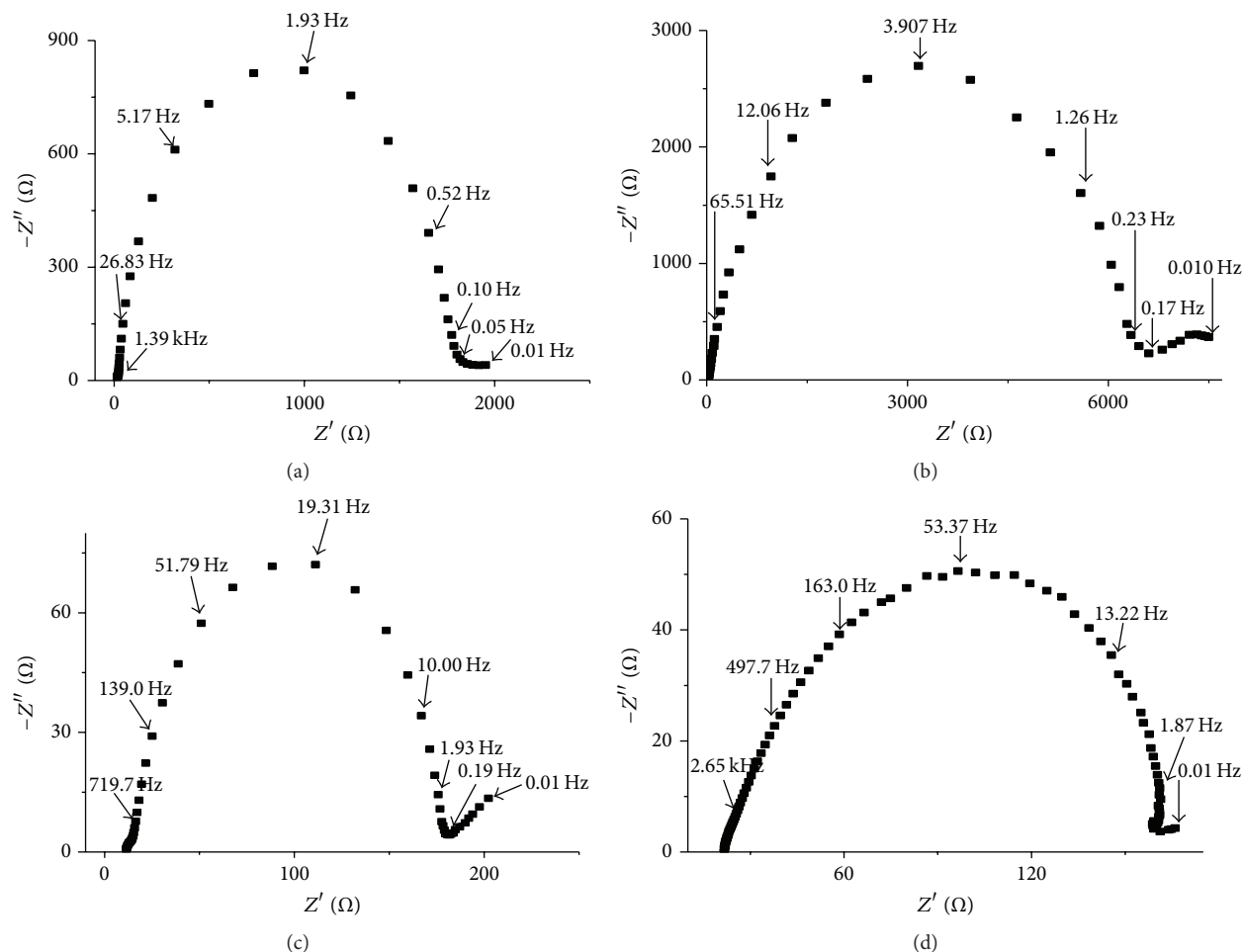


FIGURE 7: Nyquist plots for the devices fabricated with (a) ZnO alone, (b) SnO_2/ZnO with electrolyte X and (c) ZnO alone, and (d) SnO_2/ZnO with electrolyte Y under dark and forward bias at -0.58 V.

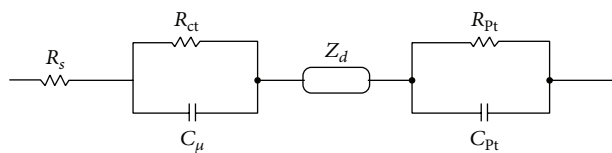


FIGURE 8: The simplified equivalent circuit of the DSCs fabricated by device structure of FTO glass substrate/ $\text{SnO}_2/\text{ZnO}/\text{dye}/\text{electrolyte}/\text{lightly platinized FTO glass substrate}$. R_s is the series resistance which corresponds to the transport resistance of the transparent conduction oxide substrate. R_{ct} and C_μ are the charge recombination resistance at the triple junctions and the chemical capacitance, respectively. R_{pt} and C_{pt} are the charge transfer resistance at the Pt/electrolyte interfaces and the interfacial capacitance, respectively, and Z_d is the Nernst diffusion impedance of the redox species in the electrolyte medium.

process. Reduction of recombination and increased dye absorption will lead to increase in the overall performance of SnO_2/ZnO composite solar cell device compared to the SnO_2 -based DSCs. Also, liquid electrolyte based SnO_2/ZnO composite solar cell device showed the best performance

compared to the other two types of gel electrolyte based DSCs. Li salt-based DSCs gave higher performance than that of the $\text{Pr}_4\text{N}^+\text{I}^-$ salt-based DSCs due to its ability of formation more amorphous gel electrolytes.

Competing Interests

The authors declare that there is no conflict of interests regarding the publication of this paper.

Acknowledgments

Financial support from the National Research Council, Sri Lanka, through Research Grant no. NRC 08-17 is gratefully acknowledged. The authors also wish to thank Professor J. M. S. Bandara of the Institute of Fundamental Studies, Sri Lanka, for granting permission to use his equipment in IPCE measurements.

References

- [1] B. O'Regan and M. Grätzel, "A low-cost, high-efficiency solar cell based on dye-sensitized colloidal TiO_2 films," *Nature*, vol. 353, no. 6346, pp. 737–740, 1991.

- [2] A. Hagfeldt and M. Grätzel, "Molecular photovoltaics," *Accounts of Chemical Research*, vol. 33, no. 5, pp. 269–277, 2000.
- [3] Z. M. Jarzebski, "Physical properties of SnO₂ materials II. Electrical properties," *Journal of The Electrochemical Society*, vol. 123, no. 9, pp. 299C–310C, 1976.
- [4] H. Wang, B. Li, J. Gao et al., "SnO₂ hollow nanospheres enclosed by single crystalline nanoparticles for highly efficient dye-sensitized solar cells," *CrystEngComm*, vol. 14, no. 16, pp. 5177–5181, 2012.
- [5] B. Onwona-Agyeman, M. Nakao, and G. R. A. Kumara, "Photoelectrochemical solar cells made from SnO₂/ZnO films sensitized with an indoline dye," *Journal of Materials Research*, vol. 25, no. 9, pp. 1838–1841, 2010.
- [6] K. Tennakone, G. R. R. A. Kumara, I. R. M. Kottegoda, and V. P. S. Perera, "An efficient dye-sensitized photoelectrochemical solar cell made from oxides of tin and zinc," *Chemical Communications*, no. 1, pp. 15–16, 1999.
- [7] G. R. R. A. Kumara, K. Tennakone, V. P. S. Perera, A. Konno, S. Kaneko, and M. Okuya, "Suppression of recombinations in a dye-sensitized photoelectrochemical cell made from a film of tin IV oxide crystallites coated with a thin layer of aluminium oxide," *Journal of Physics D: Applied Physics*, vol. 34, no. 6, pp. 868–873, 2001.
- [8] G. R. A. Kumara, A. Konno, and K. Tennakone, "Photoelectrochemical cells made from SnO₂/ZnO films sensitized with eosin dyes," *Chemistry Letters*, vol. 2, pp. 180–181, 2001.
- [9] F. Bella, E. D. Ozzello, S. Bianco, and R. Bongiovanni, "Photopolymerization of acrylic/methacrylic gel-polymer electrolyte membranes for dye-sensitized solar cells," *Chemical Engineering Journal*, vol. 225, pp. 873–879, 2013.
- [10] C.-W. Tu, K.-Y. Liu, A.-T. Chien, C.-H. Lee, K.-C. Ho, and K.-F. Lin, "Performance of gelled-type dye-sensitized solar cells associated with glass transition temperature of the gelatinizing polymers," *European Polymer Journal*, vol. 44, no. 3, pp. 608–614, 2008.
- [11] M.-K. Song, Y.-T. Kim, Y. T. Kim, B. W. Cho, B. N. Popov, and H.-W. Rhee, "Thermally stable gel polymer electrolytes," *Journal of the Electrochemical Society*, vol. 150, no. 4, pp. A439–A444, 2003.
- [12] T. M. W. J. Bandara, M. A. K. L. Dissanayake, W. J. M. J. S. R. Jayasundara, I. Albinsson, and B.-E. Mellander, "Efficiency enhancement in dye sensitized solar cells using gel polymer electrolytes based on a tetrahexylammonium iodide and MgI₂ binary iodide system," *Physical Chemistry Chemical Physics*, vol. 14, no. 24, pp. 8620–8627, 2012.
- [13] E. Stathatos, P. Lianos, S. M. Zakeeruddin, P. Liska, and M. Grätzel, "A quasi-solid-state dye-sensitized solar cell based on a sol-gel nanocomposite electrolyte containing ionic liquid," *Chemistry of Materials*, vol. 15, no. 9, pp. 1825–1829, 2003.
- [14] C. H. Ahn, J.-D. Jeon, and S.-Y. Kwak, "Photoelectrochemical effects of hyperbranched polyglycerol in gel electrolytes on the performance of dye-sensitized solar cells," *Journal of Industrial and Engineering Chemistry*, vol. 18, no. 6, pp. 2184–2190, 2012.
- [15] M. A. K. L. Dissanayake, C. A. Thotawatthage, G. K. R. Senadeera, T. M. W. J. Bandara, W. J. M. J. S. R. Jayasundara, and B.-E. Mellander, "Efficiency enhancement by mixed cation effect in dye-sensitized solar cells with PAN based gel polymer electrolyte," *Journal of Photochemistry and Photobiology A: Chemistry*, vol. 246, pp. 29–35, 2012.
- [16] N. H. Zainol, S. M. Samin, L. Othman, K. B. Isa, W. G. Chong, and Z. Osman, "Magnesium ion-based gel polymer electrolytes: ionic conduction and infrared spectroscopy studies," *International Journal of Electrochemical Science*, vol. 8, no. 3, pp. 3602–3614, 2013.
- [17] Z. Chen, F. Li, H. Yang, T. Yi, and C. Huang, "A thermostable and long-term-stable ionic-liquid-based gel electrolyte for efficient dye-sensitized solar cells," *ChemPhysChem*, vol. 8, no. 9, pp. 1293–1297, 2007.
- [18] Z. Chen, H. Yang, X. Li, F. Li, T. Yi, and C. Huang, "Thermostable succinonitrile-based gel electrolyte for efficient, long-life dye-sensitized solar cells," *Journal of Materials Chemistry*, vol. 17, no. 16, pp. 1602–1607, 2007.
- [19] P. Wang, S. M. Zakeeruddin, I. Exnar, and M. Grätzel, "High efficiency dye-sensitized nanocrystalline solar cells based on ionic liquid polymer gel electrolyte," *Chemical Communications*, no. 24, pp. 2972–2973, 2002.
- [20] W. Xiang, W. Huang, U. Bach, and L. Spiccia, "Stable high efficiency dye-sensitized solar cells based on a cobalt polymer gel electrolyte," *Chemical Communications*, vol. 49, no. 79, pp. 8997–8999, 2013.
- [21] W. M. N. M. B. Wanninayake, K. Premaratne, G. R. A. Kumara, and R. M. G. Rajapakse, "A study of the efficiency enhancement of the gel electrolyte-based SnO₂ dye-sensitized solar cells through the use of thin insulating layers," *Electrochimica Acta*, vol. 210, pp. 138–146, 2016.
- [22] W. M. N. M. B. Wanninayake, K. Premaratne, G. R. A. Kumara, and R. M. G. Rajapakse, "Use of lithium iodide and tetrapropylammonium iodide in gel electrolytes for improved performance of quasi-solid-state dye-sensitized solar cells: recording an efficiency of 6.40%," *Electrochimica Acta*, vol. 191, pp. 1037–1043, 2016.
- [23] G. R. R. A. Kumara, K. Murakami, M. Shimomura et al., "Electrochemical impedance and X-ray photoelectron spectroscopic analysis of dye-sensitized liquid electrolyte based SnO₂/ZnO solar cell," *Journal of Photochemistry and Photobiology A: Chemistry*, vol. 215, no. 1, pp. 1–10, 2010.
- [24] G. Liang, Z. Zhong, S. Qu et al., "Novel in situ crosslinked polymer electrolyte for solid-state dye-sensitized solar cells," *Journal of Materials Science*, vol. 48, no. 18, pp. 6377–6385, 2013.
- [25] S. Agarwala, L. N. S. A. Thummalakunta, C. A. Cook et al., "Coexistence of LiI and KI in filler-free, quasi-solid-state electrolyte for efficient and stable dye-sensitized solar cell," *Journal of Power Sources*, vol. 196, no. 3, pp. 1651–1656, 2011.
- [26] S.-H. Anna Lee, A.-M. S. Jackson, A. Hess et al., "Influence of different iodide salts on the performance of dye-sensitized solar cells containing phosphazene-based nonvolatile electrolytes," *The Journal of Physical Chemistry C*, vol. 114, no. 35, pp. 15234–15242, 2010.
- [27] F. Fabregat-Santiago, J. Bisquert, E. Palomares et al., "Correlation between photovoltaic performance and impedance spectroscopy of dye-sensitized solar cells based on ionic liquids," *The Journal of Physical Chemistry C*, vol. 111, no. 17, pp. 6550–6560, 2007.
- [28] J. W. Ondersma and T. W. Hamann, "Impedance investigation of dye-sensitized solar cells employing outer-sphere redox shuttles," *The Journal of Physical Chemistry C*, vol. 114, no. 1, pp. 638–645, 2010.

